Structure function Studies of Homologous Plant Lipoxygenase

by

Evan Brinkley

May 2024

Director of Thesis: Adam Offenbacher

Major Department: Chemistry

Enzymes are the catalysts of biological reactions that lower the barrier of activation energy needed for the reaction to occur. The lipoxygenase, LOX, family of enzymes is found in all kingdoms and catalyzes the oxidation of polyunsaturated fatty acids. LOXs play diverse roles in plants by affecting growth factors and pathogenic defense while human LOXs contribute to multiple inflammation pathways related to health and disease. The plant isozyme, soybean lipoxygenase (SLO), has long served as a robust model for mechanistic studies of the LOX reaction. The LOX reaction is initiated by an irreversible C-H cleavage by the LOX's non-heme, mononuclear iron cofactor. Large, temperature independent kinetic isotope effects support a tunneling mechanism for H transfer. The SLO reaction with LA is also associated with a low activation energy (E_a) whereas fungal, animal, and bacterial enzymes have displayed larger E_a values. Studies have shown a solvent-exposed loop in SLO linked to the network of thermal energy that mediates the tunneling mechanism. This same exposed loop and catalytic efficiency is not retained in mammalian LOX and is not well studied in plants other than SLO. In this thesis, a library of homologous plant LOXs is sequenced, isolated from recombinant expressions in bacteria cultures, kinetically examined, and structurally studied in reference to SLO, the model protein. This aims to examine the prevalence of efficient catalysis in homologous plant LOX while also identifying structural and sequential similarities conserved with SLO.

Structure function Studies of Homologous Plant Lipoxygenase

A Thesis

Presented to the Faculty of the Department of Chemistry

East Carolina University

In Partial Fulfillment of the Requirements for the Degree

Master of Science in Chemistry

By

Evan Brinkley

May 2024

Director of Thesis: Adam Offenbacher PhD

Thesis Committee Members:
Sambuddah Banerjee, PhD
Eric Anderson, PhD

ACKNOWLEDGEMENTS

Immediate thanks to Dr. Adam Offenbacher for creating an atmosphere of appreciating science while embracing the rigor and challenges that come with research. Thank you for your continuous support and the confidence you have instilled in me as a graduate student and in life. Thank you for being a fantastic mentor for my graduate experience and helping me see a new perspective of science.

Thank you to the Offenbacher Lab for the comradery and shared experience together. Wyatt Guy, Gage Hill, Andrew, and since-graduated Rachel Signorelli along with many other peers have made my research experience special as I have been influenced by the unique perspective each of you offer.

And finally, my family.

Thank you, Mom and Dad, for wanting the best for me under all circumstances and expressing that always. Ethan and Ryley, my brother and sister, thank you for both of your support and excitement for my field, this inspires me. I am grateful for all of you which have led me here and grateful to all who have inspired me since.

TABLE OF CONTENTS

LIST OF TABLES

LIST OF FIGURES

LIST OF SCHEMES

LIST OF EQUATIONS

LIST OF ABBREVIATIONS

CHAPTER 1 INTRODUCTION

C-H Activating Enzymes

Enzymes are well known for their remarkable catalytic ability, reducing the energetic barrier across a variety of chemical processes. The physical mechanism for understanding these catalysts has been historically based on enhanced transition state stabilization.[1] The enzymatic process is most typically contextualized through the amount of energy needed to overcome a transition barrier with E_a representing the activation energy to reach the highest transition state from the ground state moving toward the products.[2] Enzymes are known for their ability to lower the E_a needed to accelerate a chemical reaction. This enzyme-based catalysis has been shown to increase the rate of a reaction by multiple magnitudes, some reaching 10^{26} fold reaction speeds compared to the non-enzymatic reaction.[3] In Michaelis-Menten view of catalysis, the E, enzyme, and S, substrate, form together into a complex (ES) which undergoes a chemical reaction to form a releasable product (P). [1]This EP (enzyme and product complex) that is formed may dissociate its product into the environment and pick up a new substrate to take through the transition state barrier again from ES to EP.

C-H activation itself describes a sp^3-hybridized C-H bond being broken and replaced with a C-X bond where the X may be an oxygen, nitrogen, or carbon.[4] This can be done through a homolytic process where there is a formal hydrogen atom (H•) transfer or heterolytic where the proton or hydride is transferred leaving charged carbon atoms behind rather than neutral radicals in the homolytic reaction. Research in enzymatic C-H activating systems has directed some research attention towards quantum effects in the form of hydrogen tunneling to achieve such catalytic efficacy when the donor acceptor distance (DAD) is within ~2.7 Å. [5,6] This distance is

known as the tunneling-ready-state (TRS) where there is probability of wavefunction overlap between the hydrogen donor (carbon) and the accepting oxygen. The putative mechanism for the TRS revolves around the oxygen (enzyme) and carbon (substrate) being close enough that the hydrogen can "tunnel" or go through the reaction barrier. There has been a culmination of evidence suggesting that this 'tunneling' mechanism is prevalent in the macroscopic activation energy showcased by selecting C-H activating enzymes.[4] Because of the nature of tunneling, there is a breakdown of classical TST, and requires a different view of E_a.

Plant Lipoxygenase

Lipoxygenase (LOX) is an iron (typically) containing dioxygenase that catalyzes the conversion of polyunsaturated fatty acids (PUFAs) into corresponding hydroperoxides that are known as oxylipins.[7] In humans and other mammals, LOXs are associated with the body's inflammatory pathway producing the specific hydrogen peroxide products that inhibit and continue the cascade. [8] Plant LOXs are responsible for several functions in plants ranging from seed germination, plant growth, stress response, and leaf apoptosis.[9] Plant and animal LOXs generally consist of two domains: an antiparallel N-terminal β-barrel PLAT domain and a primarily helical catalytic domain **Fig 1.1**.[10] This PLAT domain has been suggested to be involved in membrane association and overall enzymatic stability. [11]

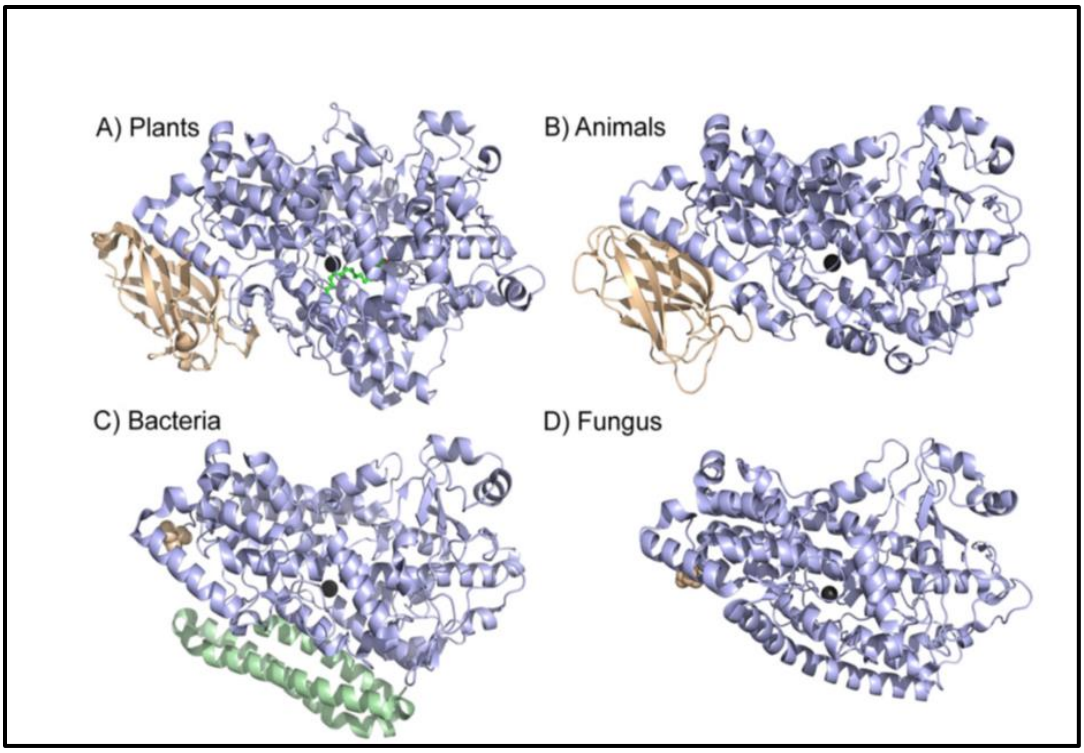

Figure 1.1. *Example of LOX Structures from each of the four kingdoms: (A) Plant (B) Animal (C) Bacteria (D) Fungus. The plant and animal PLAT domain denoted in wheat color and black metal (typically iron) core.*[10] *PDB ID: 3PZW (A), 3O8Y (B), 4G32 (C), and 5FNO (D)*

The classification of plant LOX proteins can be divided into the two categories: 9-LOX and 13-LOX, based on the site of oxygen insertion on linoleic acid (LA).[12] Additionally, 13-LOX proteins can further be categorized into two subgroups: Type I and Type II. [12]Type I 13-LOX proteins lack a transit peptide, have high sequence similarity with each other and are usually found in the cytoplasm. Type II 13-LOX proteins, on the other hand, are in the chloroplasts and have N-terminal transit peptides and moderate sequence similarity.[12]

The mechanism behind LOX's oxidation of PUFAs hinges on its rate limiting step, C-H activation. (Figure 1.2) In the case of LOX, proton-coupled electron transfer (PCET) facilitates the abstraction of H• on the *n* carbon to the metal-bound hydroxide and the electron is accepted by the metal center. As a result, the metal center is converted from a +3-oxidation state to +2 and

a delocalized radical of substrate is quenched by molecular oxygen (O_2) at either the *n*+2 or *n*-2 carbons, forming a hydroperoxide intermediate/product. [11,13,14]

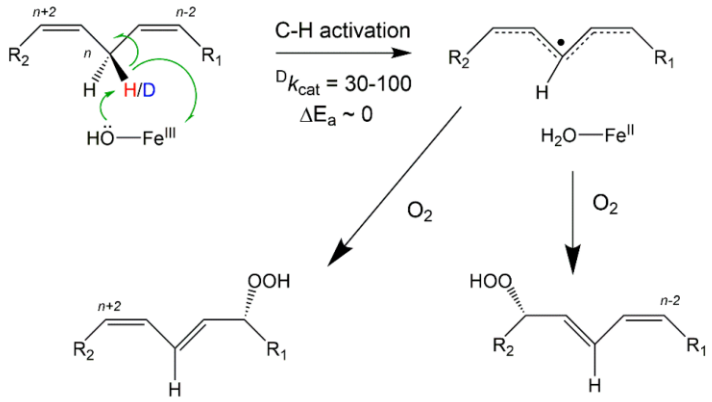

Figure 1.2: *Mechanism of plant LOX reaction Removal of a formal H atom from the substrate and formation of a radical in its place. Followed by the reaction of molecular O_2 with substrate-free radicals to generate peroxide free radicals. Select kinetic parameters (Dk_{cat} and ΔE_a) are presented for reference.*[4]

Michaelis-Menten Kinetics

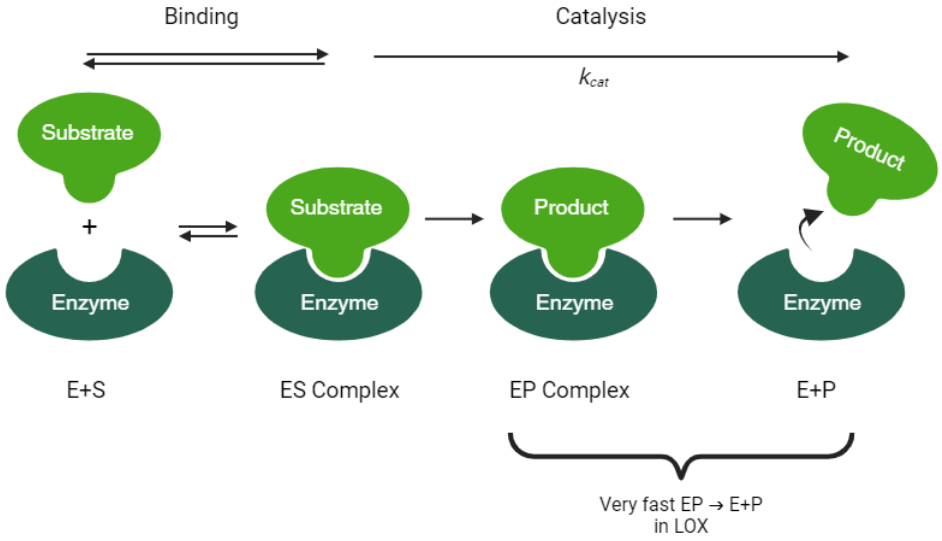

Figure 1.3. *A generalized substrate-enzyme complex illustrating the dynamics of substrate, enzyme, and product in the binding and catalysis process.*

Catalysis by transition state theory is encompassed by E+S combining to ES then transition state (ES*) into an enzyme-product complex which finally diffused into E+P. The rate of catalysis can be experimentally determined through kinetics and the Michaelis-Menten equation which relates the rate of the reaction to substrate concentration.[15] As shown in eq.1 *v* represents the velocity or rate of the reaction with given substrate concentration [S].

$$v = \frac{V_{max}[S]}{k_M[S]} \quad (1)$$

K_M represents the substrate concentration at which the reaction velocity is 50% of the V_{max} or maximum reaction velocity. K_M is a direct indication for the strength of the [ES] bound complex where lower K_M is associated with higher binding affinity while higher K_M indicates a lower substrate affinity and slower binding. Experiments surrounding K_M investigations can determine substrate preference for specific enzymes as well as inhibitor and pH studies. Using this equation, a reaction between substrate and enzyme will create a hyperbolic curve relative to the substrate concentration and rate of product formation. The first order rate constant k_{cat} and second order rate constant k_{cat}/K_m can be extrapolated from this graph as cartoonized in **Fig 1.3**. The first order rate constant k_{cat} represents the rate constant for the reaction in fully saturated substrate conditions, giving an approximate maximum rate of product formation. The second order rate constant k_{cat}/K_m reports on the proficiency of catalysis as it incorporates the substrate binding/configuration as well as product formation. The reporting of first and second order rate constants, k_{cat} and k_{cat}/K_m, provides the ability to experimentally quantify substrate affinity/binding and the effects of varying conditions, isozymes, and inhibitors on this binding.

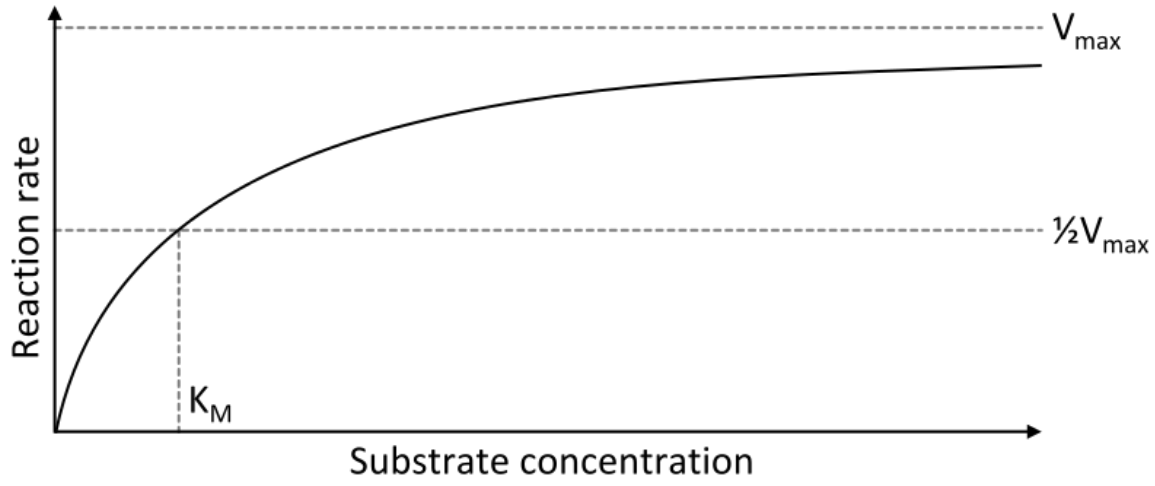

Figure 1.4. *A substrate-reaction diagram showing the V_{max} rate velocity along with its corresponding K_M at the substrate concentration of ½ V_{max}.*

The activation energy is determined from the Arrhenius equation (**Eq. 2)**, where *k* is the rate constant, T, the absolute temperature in Kelvin, A, the pre-exponential factor (constant for each chemical reaction), E_a, the activation energy, R, the universal gas constant (1.9872036 × 10^{-3} kcal·K^{-1} ·mol^{-1}.

(2) $k = Ae^{\frac{-E_a}{RT}}$

This activation energy can be quantified by observing the rate of the reaction at various temperatures ranges. An Arrhenius plot of the natural log of these rates and 1/T, where T is the temperature of each reaction, then the slope of the occurring trendline can be treated as the E_a for a given reaction type.

Isotope Effects and Quantum Behavior

As stated the LOX reaction is initiated by the cleaving of the C-H bond. To describe this step, a substitution of hydrogen for deuterium can be made. The kinetic isotope effect (KIE) can

be generally quantified as the rate constant of the lighter atom (protium hydrogen) over the rate constant of the heavier atom (deuterium). (eq 3)

Using the ratio of rate constants between the light and heavy isotope, the KIE can be established for a specific reaction type. The experimental study of primary kinetic isotope effect (KIE) can be achieved by swapping hydrogen for an isotope during the rate determining step. So, a KIE of 1 would be standard for a non-rate-limiting step which individual isotopes do not impact the speed of the overall reaction and >2 would be indicative for the hydrogen transfer being rate limiting. The upper classical limits for primary KIE within CH activation are ~7 for C-D isotopes and ~17 for C-T.

(3) $KIE = \frac{k_L}{k_H}$

H-transfer mechanism by tunneling has been well characterized in the soybean LOX-1 enzyme (SLO), this robust, model protein has become a symbol of quantum behavior in biology. SLO has been shown to have extremely high KIE, ~80, and near zero ΔE_a, which are kinetic properties indicative of quantum tunneling.[6,7,13] This kinetic isotope effect seen in SLO is far outside the bounds seen in classical transition state theory and is grounds for further investigations. Investigations have been performed displaying that C-H activation is the rate limiting step and the quenching of oxygen occurs immediately following. As seen in **Fig 1.5**, "A" represents the classical TST model of an energetic barrier which ground state reactions would cross. However, if the Donor-Acceptor-Distance (DAD) is compacted, this is known as Tunnel-Ready-State TRS and is where the hydrogen's wavelike properties can overlap between the donating carbon and accepting oxygen and transfer.

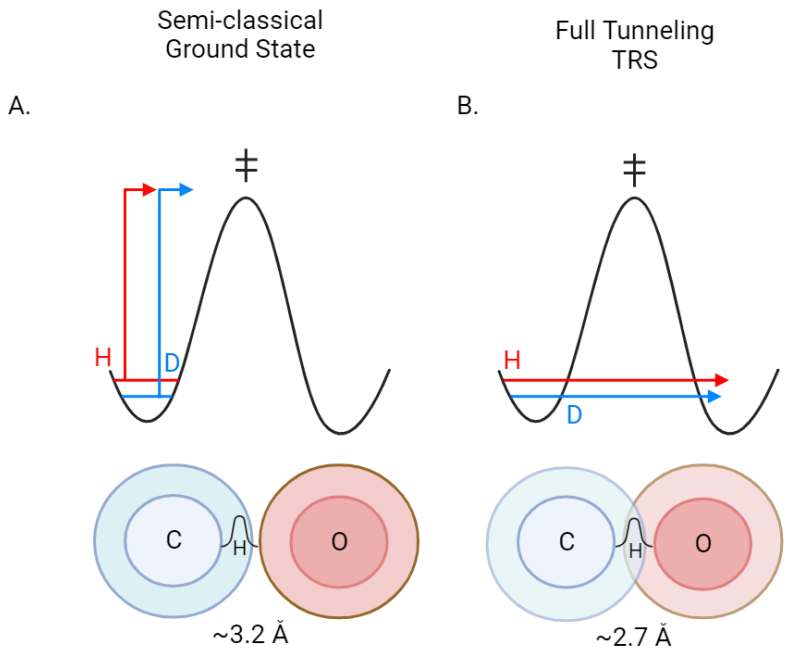

Figure 1.5. *(A) Shows a classical, ground state overview of the reaction barrier where the energy required to move over the barrier is higher for Deuterium than Hydrogen due to the difference in zero-point energies. The DAD (donor-acceptor distance) at ~3.2 is not close enough for the de Broglie wavelength of H (0.6-0.7 Å) to overlap with the C and O. (B) Shows that in the Tunnel-Ready State, the distance between the C and O orbitals allow for the wavelength of H to exist between them leading to the possibility of fully tunneling through the barrier towards the product side.*

The activation energy, E_a is the energetic potential required to cross the activation barrier (classically). In tunneling enzymes, the reaction is barrierless. In enzyme catalyzed reactions such as SLO, the observation of $E_a > 0$, indicates a role of the protein structure and dynamics to mediate close DAD. As seen in **Fig 1.4** the $\Delta E_a = E_a(D) - E_a(H)$. Under semi-classical conditions, the E_a of deuterated substrates are predicted to be higher than that of the hydrogen substrates. In a tunneling system ("B" of **Fig 4)**, the theoretical ΔE_a is zero as both the hydrogen and deuterium travel through the barrier rather than over. Soybean LOX along with preliminary evidence from other plant LOX have shown consistent, nearly temperature-independent, non-classical ranging KIE, and near zero ΔE_a. [6,7,13] Having a high primary KIE in the rate limiting

step and near zero ΔE_a is indicative of tunneling as the rate of tunneling is tied to the isotope and equally as efficient. It is expected that since $\Delta E_a = E_a(D) - E_a(H)$, that ΔE_a will be >1 if it takes more energy for the deuterated substrate to reach the activation barrier than the non-isotope. SLO, soybean LOX has become a robust model for 'hydrogen tunneling' in a biological system. Fortunately for isotope studies, the rate-limiting step of LOX's fatty acid oxidation requires the cleavage and net transfer of a hydrogen atom.

Thesis outline

SLO is already a model enzyme for showcasing thermally mediated tunneling in the active site. It is not known if this is structurally or functionally similar in homologous plant LOX where CH activation through tunneling is mediated by the same hydrophobic side chains as SLO. By studying a library of homologous plant LOX's, insights can be made regarding the pervasiveness of the active site dependent proficient catalysis.

The overarching goal of this thesis is reporting on the catalytic proficiency of plant LOX's and attempting to discern specific sequence homology, structures, and hydrophobic clusters which incentivize this behavior.

Chapter 2 of this thesis aims to cover the process of introducing this system to a CURE lab of undergraduate students in a setting which simulates a research lab experience and exposes students from biology backgrounds to quantum chemistry in nature.

Chapter 3 of this thesis explores the expression and kinetic characterization of a plant LOX library homologous to SLO which is the reference protein. Chapter 3 also uses bioinformatics to report on the relatedness in sequence and potential structure from the prospective plant LOX

library in reference to SLO. This is also factoring in the presence of kinetic characteristics and its relatedness to structural features that may mediate effective thermal energy transfer.

Chapter 2

Biological Quantum Behavior CURE

Introduction

The field of quantum mechanics is in more demand than ever with new directions and breakthroughs every year. One example of quantum mechanics in biological processes comes in the form of quantum tunneling where an object can pass through a potential energy barrier without the classical energy needed to do so. Fowler-Nordheim tunneling, named based on its discoverers, is used in most all electronics and flash memory where electrons are pushed through a thin oxide layer by voltage and allowed back by decreased voltage, thus refreshing memory in an electronic.[16] Many quantum effects necessitate extremely low temperatures for their non-classical properties to emerge. Such is seen in the case of quantum computers, superconductors, the quantum hall effect, and many others that display their quantum properties at near-zero Kelvin.[17–19] The difference in energy between discrete quantum states are exceedingly small, and when in presence of thermal energy, this difference in energy levels may be lower than the amount of available thermal energy. This means that particles can readily jump from state to state, behaving as a continuous spectrum.[20] In low temperatures where the readily available thermal energy is below the difference in discrete states, the quantum behavior in question becomes pronounced.[20] Quantum mechanics have become a “new frontier” of sorts for technologies and research in industry as well as academia, and the prospect of quantum behavior occurring at room temperature is at the forefront.[21,22] There is an overgeneralized idea that quantum mechanics are most appreciable to the fields of physics and chemistry rather than in the warm, complex environment of living organisms. This line of thought skips over the rich history

and discoveries related to quantum biology and its application to the next generation of physically applied quantum mechanics. [23–26]

In this CURE sequence, students will be exposed to and recognize the apparent effects of quantum mechanical effects associated with enzymatic hydrogen transfer reactions (i.e., hydrogen tunneling). The students will do this through the investigation of an enzyme family, lipoxygenases, which has shown some of the most compelling evidence for hydrogen tunneling in biological catalysis. Quantum mechanics has been long stigmatized as limited to the sub-atomic world, though nature has found several facets for incorporation into the evolution of biological systems.[24] Avian cryptochrome is a photo-active protein in birds' eyes which uses two entangled electrons to coordinate with the earth's magnetic field in order to migrate. [23] In photosynthesis as well, certain particles called excitons are thought to enhance the light-harvesting mechanism.[43] These examples highlight inclusion of quantum phenomena into biological evolution where species have adapted to utilize and possibly optimize the quantum mechanics inherently available.

Undergraduate Research

Course-based Undergraduate Research Experiences (CUREs) aim to integrate undergraduate research experience into a laboratory course curriculum. They allow students the opportunity to practice science and engage in science practices during their normal course of study. At most institutions, undergraduate research is primarily generated by individual students approaching labs and faculty to act on an interest they may have for the field as a career.

Additionally, CUREs give all students an opportunity to develop skills that otherwise are overlooked in traditional "cookbook" styles labs, including making an argument from evidence

obtained, defending and communicating results in a presentation or a publication, and analyzing and interpreting data [27–30]. CUREs may be considered inductive learning tools, an approach that has students use a specific method to explore a general principle, such as using UV-vis monitored kinetics to explore data collection and scientific communication. CUREs have provided gains for students in adapting important principles of science research, such as presenting research [31], confronting current trends and issues in society [32], and understanding failure as part of the scientific process[29,33]. CUREs have also provided benefits to the students outside of research skills, in areas of scientific self-efficacy—students who participate in undergraduate research, including CUREs, are shown to retain a science major and post-graduate science work for longer and with a higher likelihood of pursuing graduate studies [34,35]. Students also are more likely to self-report gains relative to those who participate in traditional labs, which indicates they were more satisfied with the skills they gained[27,36], including students from historically excluded populations. CUREs engage students with scientific skills not otherwise covered in lab courses more deeply, which has shown improvements in course DFW rates when compared to traditional labs [37] and has shown improvement in communication skills, error analysis, and data collection [38].

CUREs are being adopted in courses across many disciplines, including organic chemistry, as instructors are recognizing the benefits of teaching research skills while also teaching synthesis and other applications of organic chemistry [27,33,39]. There are examples of CUREs in sequence, as students are provided continuity between different branches of science. One example being an organic chemistry lab as the first step of a multi-course CURE where students in that course create a library of modified sugar molecules, and those who continue in the upper-level quantitative analytical CURE can evaluate the behavior of those sugar molecules. This continuity

provides the students with a vision of how chemists collaborate, how diverse chemistry work can be, and how some discoveries can lead to others[27].

CUREs have been previously developed in and reported for Biochemistry lab courses. The projects undertaken by upper-level Biochemistry students have been diverse. One involves analyzing proteins with unknown functions using software and a protein library [40], allowing students to develop technical skills, as well as thinking, reasoning, and visualization abilities by applying their biochemistry knowledge in novel situations [40,41]. The project to widely adopt this CURE, called Biochemistry Authentic Scientific Inquiry Lab, or BASIL, was utilized across eight institutions in the United States. The instructors who adopted BASIL were quick to see its benefits and were eager to share experiences at conferences. One is quoted as saying, "I hope that this research approach will become the norm" [42].

Quantum Mechanics

SLO-1 has emerged as a model protein utilizing quantum tunneling to perform its C-H activation reaction efficiently. The ease at which SLO initiates the tunneling mechanism seems to be more efficient in plants than animals, based on E_a.[2,44] This gives students in the CURE an opportunity to study a structure function relation that may span over the plant LOX kingdom. Since it is not known whether the anomalously low E_a in SLO is a common feature of all plant LOXs or a unique kinetic property to SLO, the question introduces the concept of quantum phenomena into the classroom and how it practically impacts the function of biological systems. Meaning these CURE participants are responsible for understanding the experimental design process and physically involved in the transformation, expression, and purification of multiple plant lipoxygenase (LOX) enzymes. The non-classical attributes found in SLO have not been widely tested amongst other plant LOXs, so it is not known how prevalent this tunneling behavior is

within these biological systems. This CURE offers students a chance to discover truly brand-new things in the field of biochemistry while collaborating in a team fashion.

Methodology

Context

This course is designed to be a cross-disciplinary CURE exposing undergraduate students to quantum chemistry as it relates to biological systems. This CURE sets out its cross disciplinary, cross institutional tandem project where plant lipoxygenase DNA is made into bacterial expression plasmids in a biotechnology course (BIOL 3110) led by Prof. Eric Anderson then expressed, purified, and kinetically characterized in chemistry CURE (CHEM 3771). These courses are being conducted at a Carnegie Melon Designated R2 four-year Comprehensive University which holds multiple research and doctoral programs[45.] Collaboration between the biology and chemistry departments at East Carolina University allows for the open communication and sharing of the plasmids from the biotechnology lab to be incorporated into the biochemistry CURE.

This CURE sets out a tandem project where plant lipoxygenase DNA is worked up by a biotechnology course lab taught by molecular biologist Dr. Eric Anderson. Students in this biotechnology class practice various assay and quantification techniques such as cloning plasmids, western blotting, SDS-PAGE, and ELISA (Enzyme linked immunosorbent assay). The DNA obtained from Dr. Anderson's course is then used in the CURE, led by protein biochemist Dr. Adam Offenbacher, to transform, express, and characterize the proteins acquired. Though soybean LOX (SLO) has been shown to be a robust model protein, the prevalence of the quantum behavior within other related plant LOX is not fully known. This is fertile ground for

undergraduate students to be a part of real research where they aid in or at least experience the process of discovery.

Participants

The participants in this CURE lab consists of undergraduate students mostly junior-senior level. Many of these recruited CURE participants majored in biology or a biomedical degree as this course represents a substitute for a laboratory section in biochemistry. Four total cohorts of students were formed in this lab in mostly teams of three in which they conduct their course project. Teams were formed on their own by the students and the course had equivalent student's male/female. Ethnic diversity was high within the participants with a majority of the cohorts having multiple PEERs within their team. Participants in this study also consent to surveys prior to and post the course. These surveys pose to quantify the social connections and academic progression of the students along with context for further teaching directions.

Biological Chemistry CURE

While both CUREs are important to the success of the project, the focus of this thesis chapter will on the biochemistry CURE, Quantum Effects in Biology, aims to expose undergraduate students to a team science-based research lab experience that is distinct from the typical lab course experience. Students are first exposed to background literature on hydrogen tunneling and its putative implications C-H activation reactions. With this literature review, the students are introduced to their case-study enzyme family, Lipoxygenase (LOX). Specifically in plants, LOX is known for its extremely low activation energy and elevated kinetic isotope effect, which are indicators of quantum tunnelling.

Since fall 2022, four plant LOX species *At*LOX1, *Zm*LOX5, *Zm*LOX12, and *Os*LOX1 have been studied in this course. From this DNA, they would be tasked with creating a plan to transform,

express, purify, then test their produced proteins. A team communication and research plan are made by each team and shared as a living document on Microsoft Teams for each team member to access and edit. While being exposed to protein-based biochemistry, students were taught how to navigate sequence-based tools like NCBI (National Center of Biotechnology Information) BLAST (Basic Local Alignment Search Tool), PyMOL, and AlphaFold to confirm the sequence of their protein, create predictions of their protein structure, and visualize it in PyMOL. Students were then exposed to steady-state kinetics and the use of Michaelis-Menten equations to find the rate of catalysis, activation energies (E_a), and/or kinetic isotope effects for the enzyme reaction. The characterization of the select plant LOX is evaluated using UV-vis Michaelis-Menten kinetics to determine the rate of product formation at 234 nm. For weeks, the students would be able to practice their kinetics skills with SLO as their enzyme and LA (linoleic acid) as their substrate. This was done in tandem with the actual expression and purification of their teams' target protein, so, most of the time, members of each team would take turns or split days where one would work on kinetics while the other would be responsible for the transformation, expression, or purification of their team specific enzyme. Throughout the course, students are to locate and review articles relating to quantum science applications and present the articles to the class. This offers students the opportunity to independently locate reputable scientific articles while receiving consistent feedback from their peers and educators. Each team in the course created a team presentation to highlight their research findings, with most of the teams presenting their data as PowerPoint talks and poster form in conferences outside the CHEM 3771 course.

Course Material

Students were split into teams of 2-3 where they created communication and research plan documents to be shared amongst them on Microsoft Teams. At the conclusion of the course, students were tasked with presenting their results in an oral presentation. These documents act to not only create independence amongst teams, but also to embed skills related to collaboration and how students must communicate their own teams' delegation of work. Throughout the course, each team of students express and purify plant LOXs, measure steady-state kinetics with UV/vis (Table 2.1).

Table 2.1*. This table shows the various attributes of a complete CURE lab and their applications within the CHEM 3771.*

CURE	CHEM 3771: Quantum Effects in Biology
Research Practice	Bacterial transformation, UV-Vis data collection, protein purification via Ni^{2+} columns, steady-state kinetics
Discovery	Expression and characterization of non-characterized plant LOX and mutants related
Relevance	Quantum behavior, especially in biological systems at room temperature, is forefront science
Collaboration	Fall 2022: 3 teams of students with each team keeping a research plan, communication plan, and lab notebook shared. Fall 2023: 1 team of students working to kinetically characterize mutations in *Os*LOX1
Iteration	Students were given many opportunities to practice and receive triplicate kinetics data along with numerous low-volume pipetting practice

Survey

In the first and final week of class, students are given survey of the quantum mechanics terminology where they will record their comfortability with the subject on a scale of 1-3 (1 being unfamiliar or not knowledgeable and 3 being confident/mastery). There is also a final question asking students to think about applications of quantum mechanics and how it is related to a real-world example. The goal of this assessment is to give a baseline for recognition of quantum phenomena. It is possible for undergraduate students (especially non-senior) to have

little to no prior knowledge of quantum science until this course due to the infrequency of quantum behavior taught as course focal point. The final survey seeks to identify any growth of information of quantum science. These are compared to a sister course 3770 where quantum mechanics are not explicitly taught.

Skills Assessment

Students in this CURE are given various pre-survey/assessments, conceptually and practically. On the first day of lab, students are given a brief survey to assess their confidence over certain quantum mechanics concepts. This includes a free response question asking students if they knew of any real-world applications. This assessment is then again given in-post or at the end of the semester for the students to complete again. The first week of lab also granted the opportunity to demonstrate pipetting for the first time. The students tracked the µL they expected to pipet and the recorded weight they receive. 1 mL of water = 1 g, so students can calculate how far their expected volume is from the actual amount on the scale. For characterizing enzyme kinetics, a fair amount of practice is needed to get precise and accurate kinetic rates for enzyme reactions. Within the first 2-3 weeks of class, students are tasked with doing Michaelis-Menten kinetics for a full substrate concentration range, using SLO reaction with LA as a standard. The values they get for this exercise serves as practice and to be compared with some of their data later in the semester. Familiarity with pipetting techniques and identifying amino acid sequences are regular practice in the biochemistry field, so early developed habits and skills can shape the progress of an individual student's science career.

Transferable Lab Techniques

Students in this course may gain their first experiences working with protein expression and purification. Students are to understand how to design the primer and mutation process using polymerase chain reaction.

There is considerable practice with steady-state kinetics throughout the course. In the first few weeks, students begin gathering Michaelis-Menten substrate-enzyme concentration curves at room temperature. These graphs serve to display progress in proficiency over the semester, and an averaged baseline of their (3) best trials for wildtype proteins to compare with their mutant studies. In semesters of this CURE where there are no mutants, students practice with SLO to be compared with the kinetic studies of homologous plant LOX from other species. Students gain familiarity with UV-vis spectroscopy and Beer's Law.

Results and Discussion

Survey Results

The quantum topics survey that was given at the start and closing of the semester gives students an opportunity to assess their own comfortability with terminology that they are likely exposed to in general courses as well as more specific terms found commonly in advanced physical chem courses. (Fig 2.1.)

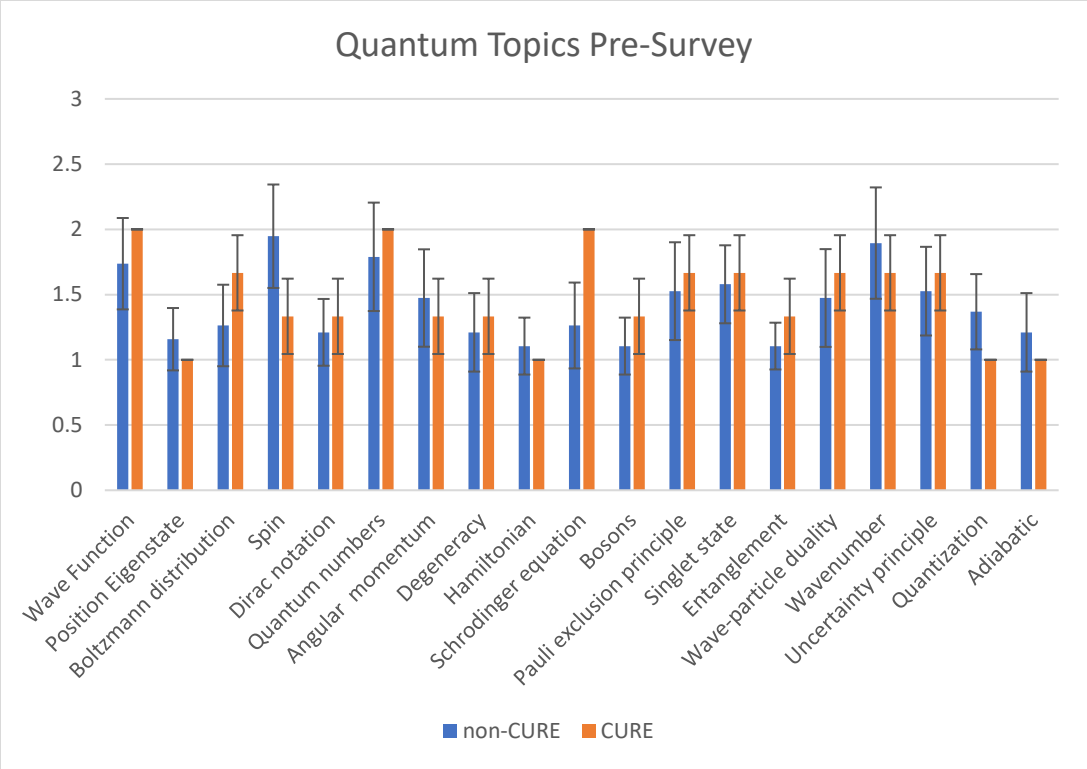

Figure 2.1. *The above bar-graph shows the results of their comfortability with the subject on a scale of 1-3 (1 being unfamiliar or not knowledgeable and 3 being confident/mastery) during the beginning of the semester.*

The pre-surveys between the CURE and CHEM 3770 sample are based only on students' previous knowledge and acts as a baseline for comparison. Perspectives for variance could include students with more "hobby" knowledge on subjects may be more, or less, inclined to participate in CURE courses. With this, spin and wavenumber stood out in the pre-survey data as non-CURE students ranking higher average comfortability with the subject than CURE students. However, the CURE students sample size is very small (n=3) compared to the non-CURE (n=21). Certain topics like the Schrodinger equation are recognized consistently with the CURE sample while less so in the non-CURE.

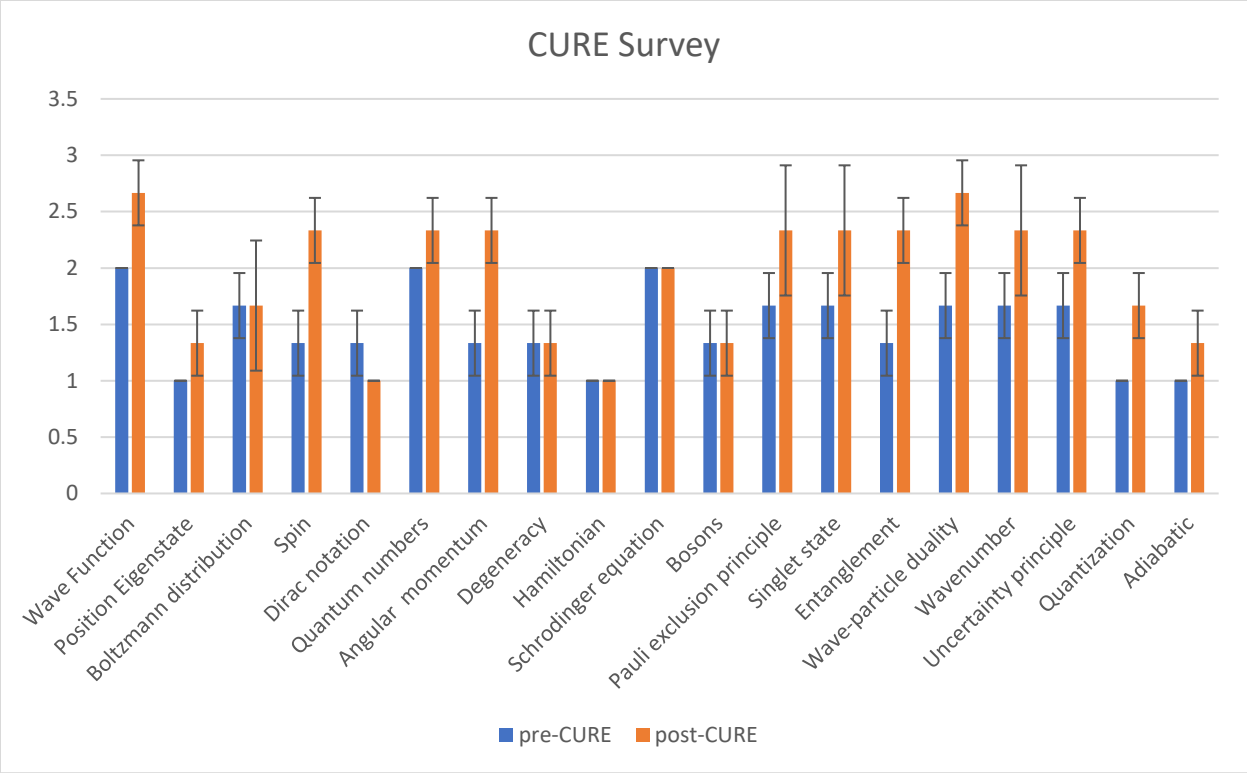

Figure 2.2. *The above bar-graph shows the results of the CURE students' comfortability with the subjects from the start to closing of the semester.*

From the quantum topics mentioned, the CURE sections had the highest reported comfortability with wave functions and wave-particle duality. This result seems intuitive to the chronological order a student might gain comfortability with quantum subjects. Certain subjects such as Hamiltonian and Dirac notation had the lowest reported comfortability in the CURE sections, pre and post survey. This can be rationalized from the specific subjects not being extensively covered in the course as other topics that were much closer related to the course work going on in lab. Topics like entanglements and wave-particle duality showed greatest increase in comfortability which is a result intuitive to the amount the subjects were related to the CURE course content.

Student Course Achievement

Students in the CURE course have expressed various plant LOX from bacterial cultures. Throughout the course, four plant LOX's (*At*LOX1, *Zm*LOX5, *Zm*LOX12, and *Os*LOX1) have been expressed and purified. Through kinetic characterization, it was shown that *Zm*LOX5 had low activity, thus three functioning enzymes were expressed by four teams of undergraduate students over two semesters. A mutant of *Os*LOX1 was also expressed by the Fall 2023 CURE team with little activity compared to wildtype.

Kinetic Studies

Michaelis-Menten kinetics was performed by undergraduate students in the CURE to report on potential quantum tunneling features in plant LOX.

In the fall 2022 semester, the three teams of students performed Michaelis-Menten kinetics at 4 temperatures (10,20,30,40°C) to extrapolate a putative activation energy for their specific LOX species. From these student experiments, *Zm*LOX12 was decided to be set to the side as it was shown to have extremely low activity. This type of experience is important for students as they realize the unpredictability of research and how to change directions of experiments based on the data received. *Zm*LOX5 is another LOX species from the same *Maize* family, the team responsible for kinetic reporting on *Zm*LOX5 found the E_a to be ~5.9 kcal/mol. Another team in the same semester worked up *At*LOX1 and performed the same temperature based Michaelis-Menten experiments; they reported an E_a of 13.52 kcal/mol. This reporting seems elevated compared to other kinetic testing performed on *At*LOX1. Some issues in precision may have arisen due to different team members being responsible for different temperatures in the aim of a collaborative Arrhenius plot with the k_{cats} from each temperature.

Chapter 3

Plant LOX Library

Introduction

SLO has been shown as a robust enzyme exhibiting low activation energy (2.1 ± 0.2).[44] Mammalian LOX's have an E_a of ~8-12 which is notably higher than that of SLO. [44] This opens the door for the kinetic investigation of homologous plant LOXs. Is the near zero E_a and nearly temperature independent kinetic isotope effects also present in other plant LOX or is this exclusive to SLO? In order to examine this point, a library of diverse homologous plant LOX needs to be worked up and kinetically characterized. The LOX family has notoriously low sequence identity to even closely related homologues, for this reason, sequence alignment and phylogeny studies are first conducted to quantify the diversity of plant LOX and their relation to SLO and each other. From this library, which was prepared in part from efforts from the Biotech CURE lab (see Chapter 2), I characterized the kinetics of these LOXs with LA.

Materials and methods

Plant LOX expression and purification

*At*LOX1, *Zm*LOX5, *Zm*LOX12, and *Os*LOX1 plant LOX genes are encoded into a pET28 expression vector in line with an Ni-terminal hexahistidine (His6) tag. and are used in a transformation with *E. coli* BL21(DE3) Codon Plus RIL competent cells for protein expression. The cells are transferred into Kanamycin-containing LB starter media and allowed to shake

overnight at 37 °C. The overnight starter culture is then transferred into 2 8L Fernbach flasks with 0.8 L 2xYT enriched media, and KAN. The cultures shake at 37 °C until the optical density (OD_{600}) reaches around 0.9-1.0, then the temperature is decreased to 18 °C for continual shaking for up to 40 hours. The cultures are then centrifuged at 10,000 x g for 5 minutes to pellet the cells. A lysis buffer is prepared (milli Q water, 50% glycerol, 0.5 M $NaPO_4$, 0.5 M NaCl, and 20 mm magnesium sulfate.) ~10 mg lysozyme, ~ 4 mg DNAse to remove unwanted DNA from the cell lysate, and ~20 mg AEBSF-HCl, to inhibit proteases from breaking apart peptide bonds during purification, are then added to the lysis buffer along with the cell pellet and allowed to stir. The cell suspension is then put on ice and sonicated 3 times on and off for 5 minutes each. The sample is centrifuged again at 18000 x g for 20 minutes and the supernatant is transferred into a 250 mL flask on ice to resuspend the nickel column in.

The proteins are purified using a Ni-NTA gravity column to capture the histidine-tagged LOX. The column containing the lysate mixed and stirred with the column then, after flowthrough, washed with buffer A (20 mM Tris-HCl, 20 mM imidazole, 500 mM NaCl, pH 8.0) to remove contaminants, and the LOX of interest is eluted off the column with buffer B (20 mM Tris-HCl, 200 mM imidazole, 500 mM NaCl, pH 8.0). The protein is confirmed with UV-Vis spectroscopy for presence of protein (280 nm) and SDS-PAGE. SDS-PAGE (sodium dodecyl sulfate polyacrylamide gel electrophoresis) is a separation technique that separates proteins based on their size. It can be used to confirm the purity of the protein by checking if there are any contaminants or other proteins present in the sample. The protein of interest should appear as a single band on the gel if it is pure. A PD-10 column is used to exchange proteins into the storage buffer (50 mM HEPES, 150 mM NaCl, pH 7.5), frozen in liquid N2, and stored at -80°C until further use. Additional purification steps may be taken to enhance the purity of LOXs

following the Ni-NTA column.

Kinetics

The LOX reaction (enzyme with varying concentrations of substrate, LA) is monitored continuously at 234 nm using a UV/Vis spectrometer with an attached VWR digital temperature-controlled circulating water bath to keep the reaction at a constant temperature. The enzymatic activity and calculated velocity are first found for each of the 6 substrate concentrations (5, 10, 20, 25, 50, 100 µM) at a constant temperature to determine the kinetic parameters (k_{cat} and K_m) and varying pH values at 25°C: 6,7,8 and 9 to find what the optimal pH was for each protein's enzymatic activity. The same experiment can then be done with a constant pH (optimal) buffer and varying temperature range (10, 15, 20, 25, 30, 35, and 40 °C). Fitting this graph to the Michaelis-Menten equation in the data analysis program, Igor Pro, calculates the k_{cat} and Km for the given temperature set. The resulting k_{cat} values are used in the Arrhenius equation. Temperature and k_{cat} are graphed with $\frac{1}{T}$ on the x-axis where T is temperature and ln (k) on the y-axis using the k_{cat} of each temperature. The slope of this graph will be $-\frac{Ea}{R}$, and the activation energy can be easily determined based on the ideal gas constant 1.98 cal/mol K.

Kinetic Isotope Studies

Kinetic isotope effects are determined from the first and second order rate constants when HLA and DLA substrate are studied. LA (HLA) and DLA refer to the natural abundance and deuterium labeled substrates, respectively. From here, experiments are run testing the difference in Michaelis-Menten kinetics based on the deuterated or non-deuterated substrates. To calculate E_a and ΔE_a, temperature-based studies of HLA and DLA are performed at 10, 15, 20, 25, 30, 35, and 40 °C. The catalytic difference between HLA and DLA is then ready to be compared and E_a

of each are used to calculate the ΔE_a which is a useful metric in quantifying quantum effects.

Structure Predictions

AlphaFold, on its own, is a Google owned company with a website that acts as a database for previously generated or experimentally determined protein structures.[46] In addition to this, the source code for AlphaFold's artificial intelligence is public, meaning that it can be accessed through Google Drive on a 'Google Colab' document. A single amino acid sequence can be entered for the monomer model, and multiple amino acid sequences can be added if a multimer model is desired. AlphaFold first aligns the amino acid sequence of the protein with the sequences of related proteins that have known structures. The Clustal algorithm is used to perform this sequence alignment, which helps to identify the conserved residues (amino acids) in the protein of interest. The conserved residues are then used as landmarks to guide the prediction of the protein's structure. The Clustal algorithm works by constructing a distance matrix for the sequences being aligned, which measures the similarity between each pair of sequences. The algorithm then uses this distance matrix to build a guide tree, which represents the evolutionary relationships between the sequences. Finally, the algorithm aligns the sequences by following the branches of the guide tree, starting with the most similar pairs of sequences, and working up to the least similar pairs. Finally, five models are produced and ranked by the lDDT score and PAE maps to assess inter-domain accuracy. Local Determinate Distance Tests are made with the AlphaFold structures, and they give a superposition free score of higher and lower confidence residue areas of the generates structure. PAE maps are cross sectional illustrations which indicate the expected positional error at residue x if the predicted and actual structures are aligned on residue y.

A predictive protein structure for each LOX was developed using AlphaFold by creating 5

models for a single protein and undergoes analysis to rank and determine the accuracy for each. Predicted lDDT charts and a PAE map are created for each protein model to be ranked. The rank 1 predicted model for each protein will be used as the putative predicted structure for LOXs without crystalized structures resolved (PDB ID: 3PZW, SLO-1). *Zm*LOX5 (ABC59688), *Os*LOX1 (ABF98382.1) The local Distance Difference Test (lDDT) is a way of evaluating a superposition-free score for the distances of individual atoms within a model and the stereochemical plausibility of the structure. This test uses either a singular reference model or a collection of similar structures from the given database, thus allowing lDDT to emerge as a robust tool for the automated assessment of structure predictions.[47]

Results

Sequence alignment and SDS

Clustal sequence alignment and NCBI's BLAST (Basic Local Alignment Search Tool) was used to quantify the sequence similarities across the various plant LOX. Protein's along with their genebank accession number were searched and compared to get a percent identity to each other. By using Omega Clustal, a phylogenetic tree was resolved to compare the relatedness of the LOX library.

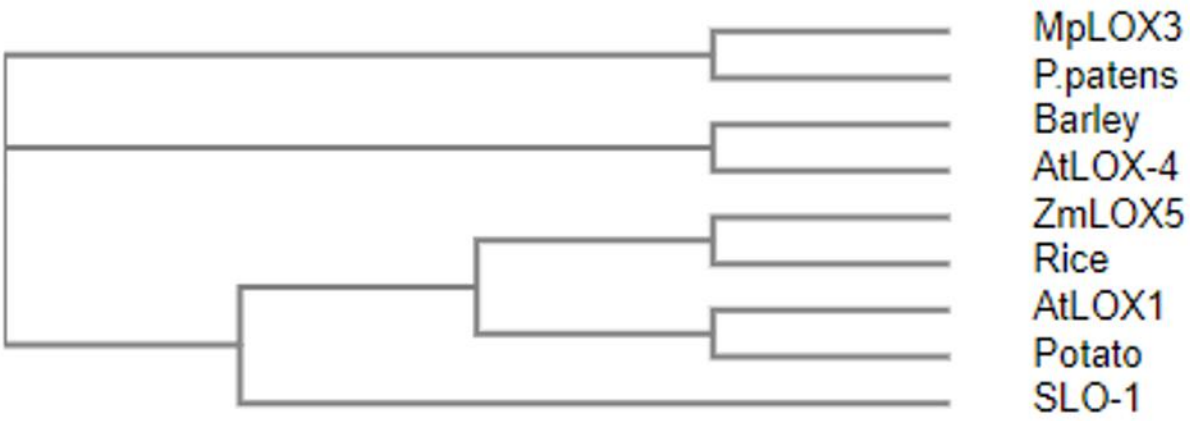

Figure 3.1. *Above shows the phylogenetic diversity amongst different LOX species from sequence alignment of a library of various LOX species. MpLOX3 (BAJ46516.1) P.patens 13-LOX (ABF66650.1), Barley LOX2 (spP93184.1), AtLOX4 (spQ9FNX8.1), Rice LOX1 (ABF98382.1), Potato StLOX (P37831)*

Omega clustal's phylogenetic tree is based on an algorithm which denotes relatedness within the available sequences based on each other. In **Fig 3.1.** the right-hand numbers are to denote the relatedness of each species where closer numbers show higher relatedness. Omega clustal also denotes potential probable nodes based on the difference in relatedness and shared sequence between proteins.

pH Effects

Each enzyme's optimal pH and salt affinity were determined through duplicate studies at a constant temperature (25 C) finding the highest activity (rate of catalysis k_{cat}) with lowest K_m. The pH activity at each LOX *At*LOX1, *Zm*LOX5, and *Os*LOX1 were kinetically characterized from pH 6 to 9, by single pH units. The optimal pH for SLO was previously found to lie between 8 and 9, in agreement with previous publication.[48] *Zm*LOX5 showed its highest k_{cat} at pH 8, though the K_m was elevated at this pH compared to at pH 7 where the k_{cat}/K_m was the greatest.

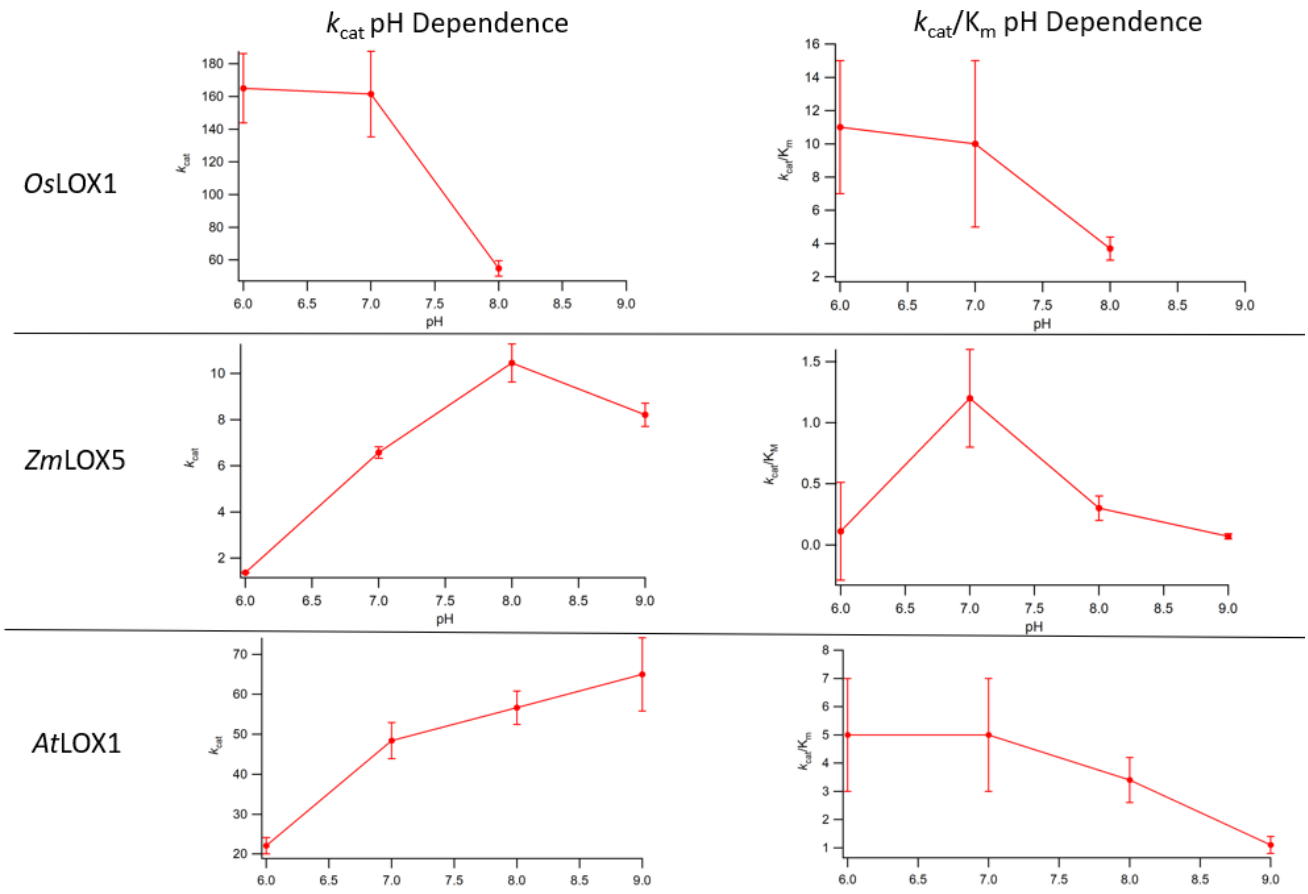

Figure 3.2. *Above shows the effect of pH on the k_{cat} and k_{cat}/K_m for OsLOX1, ZmLOX5, and AtLOX1 at 25°C.*

pH studies of *At*LOX1 showed the highest activity and k_{cat}/K_m at pH 7 as well as a salt affinity which lowered the K_m. In *At*LOX1, there is a steep drop in efficiency in higher pH's. *Os*LOX1 pH dependance showed that pH 6 and 7 had equivalent kinetic values so pH 7 was continued.

Kinetic Parameters

As shown in **Table 3.1**, the first order (k_{cat}) and second order (k_{cat}/K_m) rate constants of *At*LOX1, *ZmLOX5, Os*LOX1 act as kinetic comparison to (control) SLO studies. Using the optimal pH

conditions, the k_{cat} of SLO is the highest of all plant LOX studies, though the k_{cat}/K_m was similar in range to *Os*LOX1. *Os*LOX1 and *At*LOX1 showed a higher rate of catalysis (k_{cat}) than *Zm*LOX5 with *Os*LOX1 being the most active plant LOX homologue tested. The rate of catalysis for deuterated substrate versus non-deuterated substrate grants the KIE value for the specific enzyme. ZmLOX5 had rather low activity regardless, so AtLOX1's and OsLOX1's KIE was found. The KIE for OsLOX1 was 80 ± 10 and for AtLOX1 40 ± 10. Both of which are greatly elevated compared to classical standards, indicative of tunneling.

Table 3.1. *Below shows a table of kinetic parameters for each of the plant LOX characterized.*

LOX Species	KIE	K_m @25 °C	k_{cat} @25°C	k_{cat}/K_m @25°C	E_a kcal/mol
SLO	~80	28.3 ± 3.9	292.3 ± 16.7	10.3 ± 1.5	2.19 ± 0.4
***At*LOX1**	80 ± 10	24.2 ± 4.0	87.4 ± 5.7	3.6 ± 0.6	5.33 ± 0.9
***Zm*LOX5**	---	28.4 ± 6.0	10.6 ± 0.9	0.4 ±0.1	0.91 ± 0.4
***Os*LOX1**	40 ± 10	13.0 ± 11.5	113.5 ± 11.5	8.7 ± 7.7	1.12 ± 0.5

Activation Energies (E_a)

Temperature based kinetics were run from 10-40°C, by 5°C increments, to determine the E_a for each of the plant LOX. The E_a of *Zm*LOX5 and *Os*LOX1 are comparable with the determined E_a for SLO ≤ 2 kcal/mol. *At*LOX shows a slightly elevated E_a of 5.3 +/- 0.9 kcal/mol.

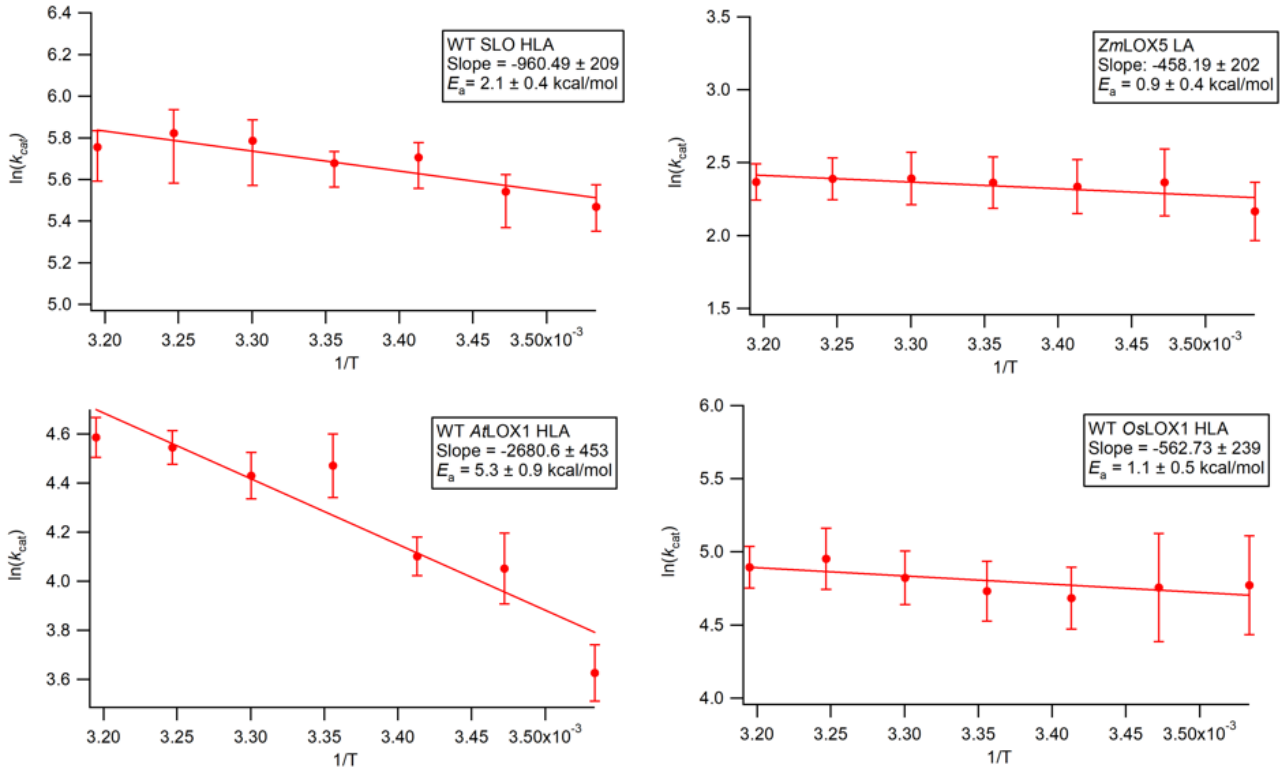

Figure 3.3. *An Arrhenius plot for (A) SLO (B) ZmLOX5 (C) AtLOX1 (D) OsLOX1 where the y-axis is formed from the natural log of each temperature's* k_{cat} *while the x-axis displays 1/Temperature. The slope of the trendline is a function of the* E_a *and can be calculated.*

The E_a values of the plant LOX library (*At*LOX1, *Zm*LOX5, and *Os*LOX1) have all been shown to be 1-5 kcal/mol, which is considerably lower than animal LOX activation energies, (8-13 kcal/mol). *At*LOX1 showed the highest E_a of the plant LOX tested (5.3 ± 0.9). This is still distinct from animal LOX which generally has E_a's of 8-12.[49] These data provide evidence that the low *E*a in SLO is a conserved kinetic feature for diverse plant LOXs and distinct from animal LOXs.

Discussion

Thermal Loop and Hydrophobic Clusters

The origin of the anomalously low E_a in SLO is centered around the active site compacted TRS (tunnel ready state). This tunneling mechanism seems to be enabled by thermal energy causing efficiency of the protein thermal motions in facilitating close compaction of the DAD to promote effective tunneling. HDX and other experiments of SLO has shown a surface loop from residues 317-334 that demonstrate direct link between protein thermal motions and the activation barrier for catalysis.[44] This "thermal loop" is not shared amongst mammalian LOX's, though it is not known how pervasive this "thermal loop" is in other plant LOX homologues except SLO. The distinctly low E_a seen in plant LOX and their extremely efficient catalysis may be related to the protein motions made by the loop. If the "thermal loop" is prevalent amongst the plant kingdom along with its notably lower E_a then it may be indicative of a different, more efficient activation of their tunneling mechanism compared to mammalian LOX counterparts.

Using AlphaFold, predictive structures of the plant LOX library have been generated to be structurally compared. The validity of each AF2 structure was determined by comparing the X-

ray solved SLO structure to the model generated by AlphaFold.

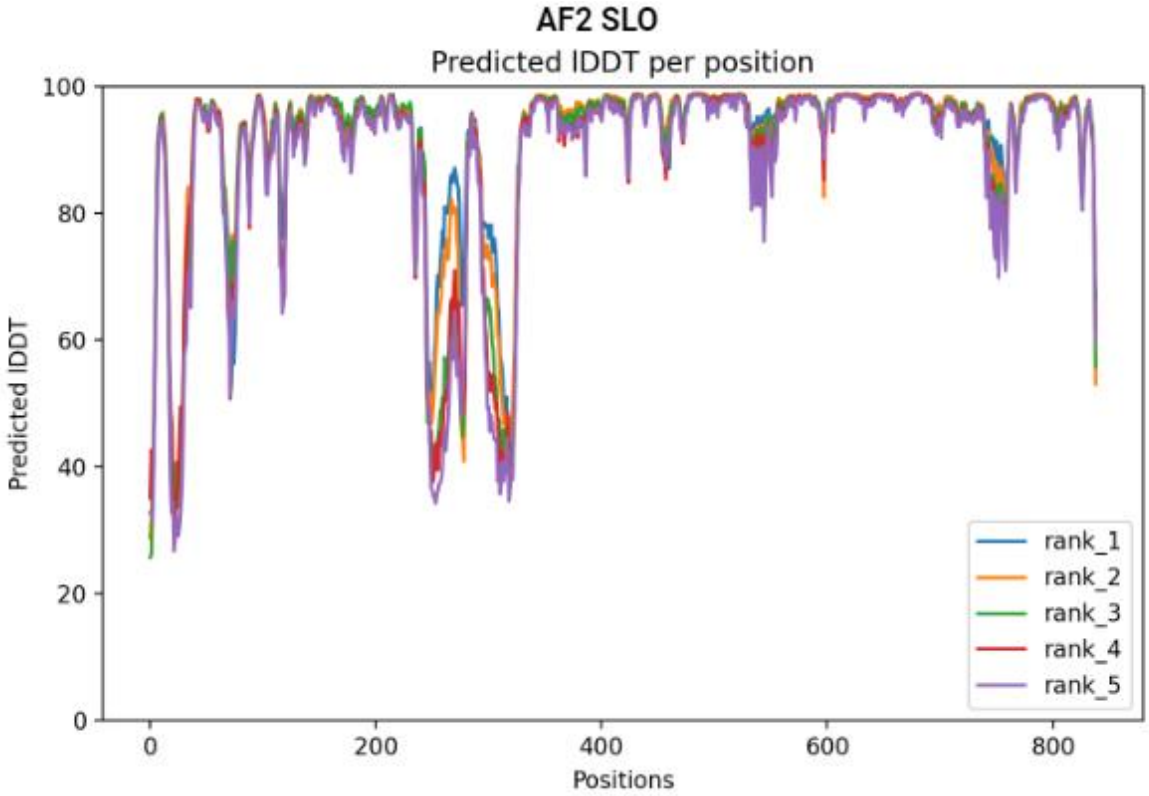

Figure 3.4. *Example lDDT for the AlphaFold generated structure of SLO showing the confidence of predicted structure based on amino acid position. This is to be compared with the known SLO crystal structure to understand where the predicted structure commonly misaligns with the crystal reference structure.*

As mentioned, in an x-ray resolved SLO structure, the 'thermal loop' is situated in residues 317-334 which is reflected with reduced confidence in the predictive model. Other notable reduced predictive scores relate to the N-terminus PLAT domain and the catalytic domain's Alpha helix 2 before the thermal loop.

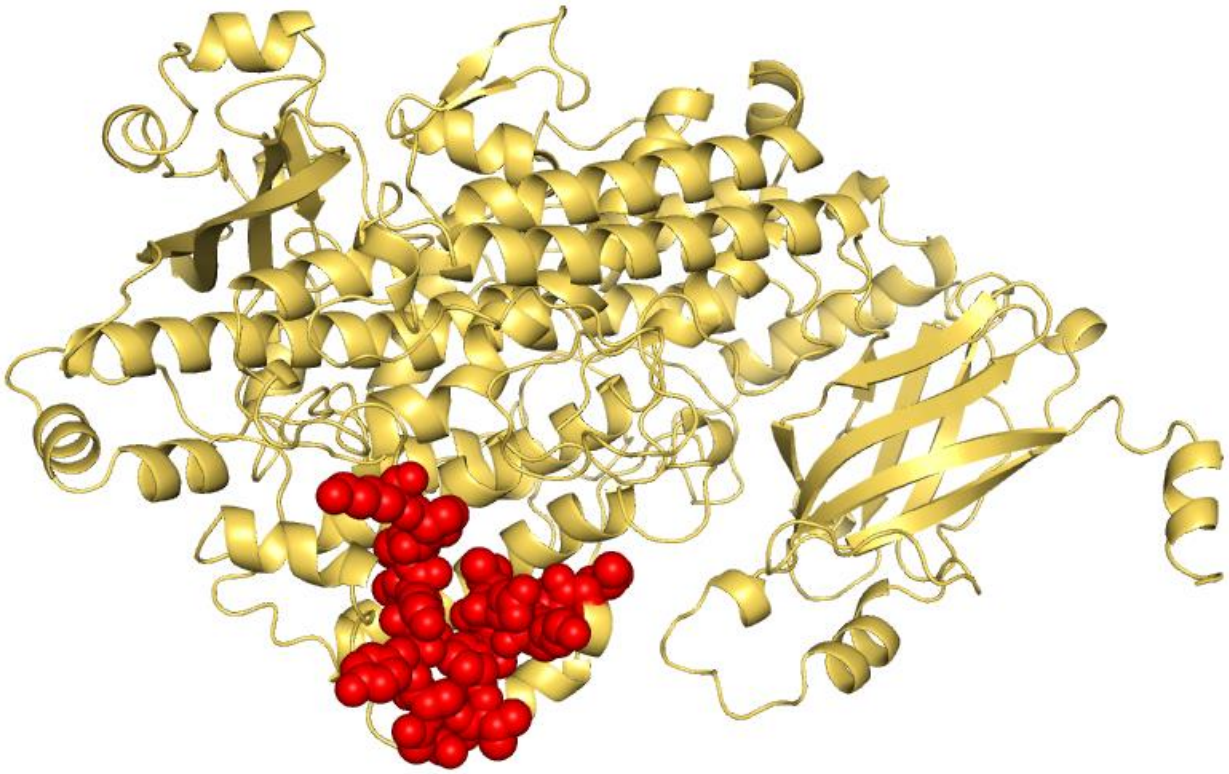

Figure 3.5. *AF2 OsLOX1 with residues 329-350 (red spheres) correlating with the thermal loop resolved in SLO.*[44]

In the predictive models for the plant LOX library, a string of residues are conserved similar to the thermal loop identified in SLO.[8] For example, in mammalian LOX, human 15LOX-2 (4NRE) is 145 less amino acids in sequence compared to SLO (3PZW) and does not contain the same thermal loop seen in figure 3.5. The homologous thermal loop is conserved in the predictive structure of *Os*LOX1, *At*LOX1, and *Zm*LOX5 which have all been kinetically examined.

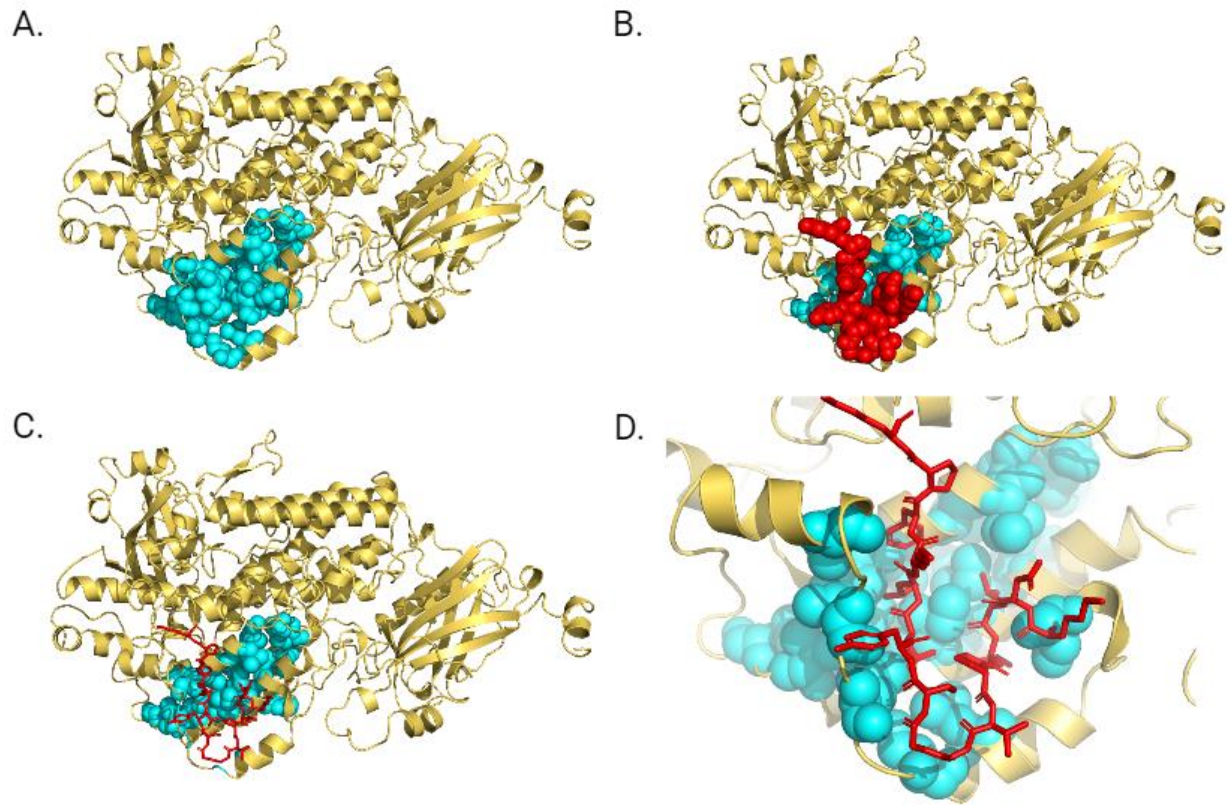

Figure 3.6. *AF2 generated OsLOX1 structure with the putatively conserved 'thermal loop' (red) and corresponding ILV hydrophobic cluster (cyan). (A) Cluster 6 (cyan spheres) in the predictive OsLOX1 structure alone (B) Overlay of (C) (D)*

Furthermore, the thermal network in SLO was found to have a high propensity of Ile, Leu, and Val (ILV) sidechain clusters. ILV hydrophobic cluster maps of the plant LOX library were generated using ProteinTools Contacts of Structural Units (CSU). An ILV HC of a crystal structure of SLO (3PZW) was compared with the predictive protein structure of SLO to first gauge the disparity between AlphaFold generated models and crystal structures.

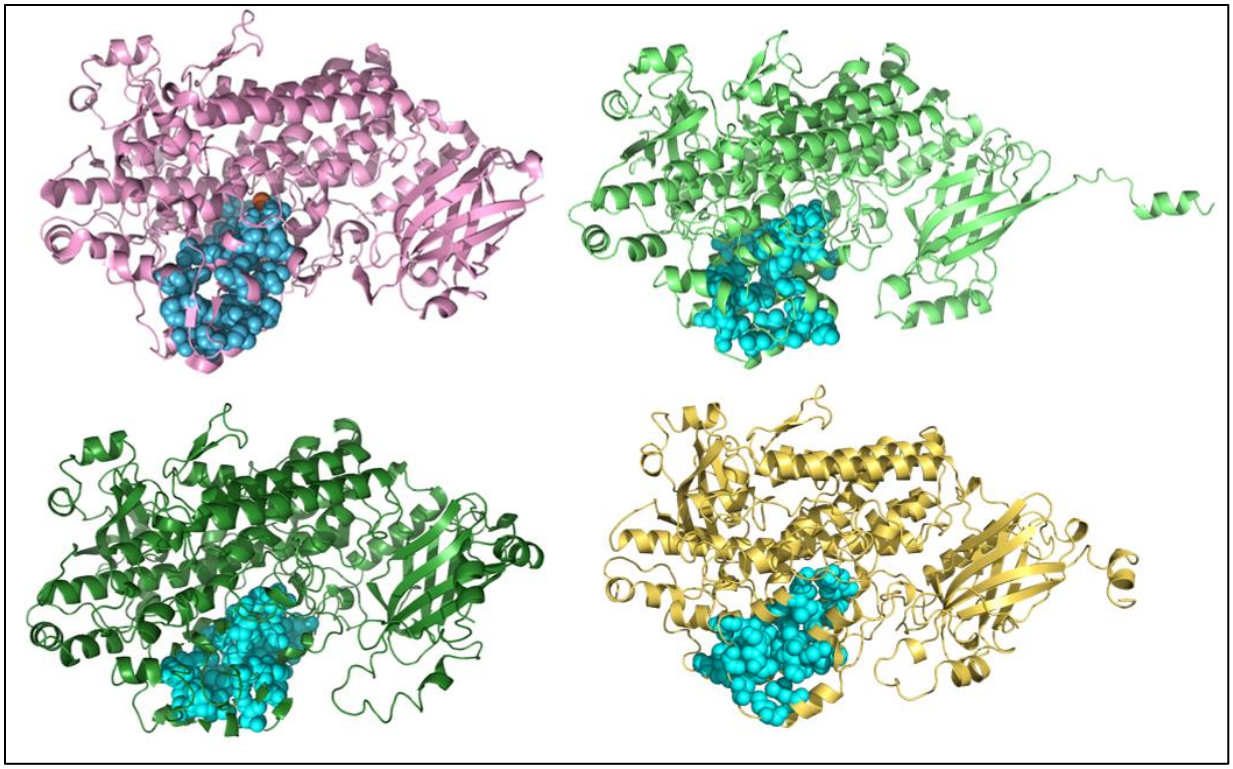

Figure 3.7. *Crystal 3PZW SLO (Pink). AF2 generated: AtLOX1(Light Green), OsLOX1 (Yellow), ZmLOX5(Dark Green) structure with the largest respective ILV hydrophobic cluster (Cyan) putatively conserved 'thermal loop' (red)*

Table 3.2. *Below shows the largest ILV hydrophobic clusters for each AF2 generated plant LOX library in reference to the x-ray resolved SLO (3PZW)*

Plant LOX	Cluster ID	Area	Number of contacts	Contacts/Residue	Area/Residue
SLO (3PZW)	5	4253.29	96	3	44.31
AF SLO	6	5134.71	107	2.97	47.99
AF *At*LOX	6	5105.68	117	3.55	43.64
AF *Zm*LOX	10	4712.07	97	3.23	48.58
AF *Os*LOX	13	5310.47	101	3.37	52.58

The largest area ILV found within the predictive and crystal structure corresponds to a looplike structure that facilitates thermal energy in the form of protein motions. Between 3PZW and the AF-SLO, there were the same number of ILV hydrophobic clusters while slight differences in predicted area of such residues. It is important to note that between ILV HC predictions on the same PDB model, the cluster areas can vary slightly as well, and the area of the AF cluster was 20% greater than the crystalized model (5134.71Å and 4253.29Å) This gives foundation and reference for the other predictive plant LOX structures and their ILV mapping. Each of the plant LOX library (*At*LOX1, *Zm*LOX5, and *Os*LOX1) have their largest cluster in the same physical region of the protein, in the previously mentioned "thermal loop" found in SLO. Now that this conserved loop-like structure has been identified in homologous species with similar kinetic traits, the effects of certain mutations in this loop may show impact to the efficiency of catalysis.

Summary

From the plant LOX library expressed and kinetically characterized so far, the low E_a seen in SLO is retained. ***Table 3.1.*** The KIE of *At*LOX1 and *Os*LOX1 are both multiple times higher than the classical limit which is indicative of conserved tunneling mechanisms. In addition to the kinetic similarities between SLO and the other plant LOX species, the largest ILV cluster in each LOX occurs in the same region. In SLO, this ILV hydrophobic cluster correlates with its solvent-exposed 'thermal loop' which putatively mediates thermal energy to the active site. In sequence alignment and structure study between SLO and the homologous plant LOX, the (position 317-334) thermal loop in SLO is conserved in the same region in the other plant

LOX. ILV cluster analysis on the plant LOX library also showed their thermal loop being correlated with their largest ILV cluster, as also seen in SLO.

Experiments can now probe into the effects of certain residue mutations in the homologous ‘thermal loop’ of non-SLO LOX. Since the tunneling aspect of the reaction being a net bypass of the activation barrier, the E_a of a reaction is on held to the initiating of the tunneling itself. The thermal network seen in SLO is highly efficient in its evolutionary direction towards utilizing a tunneling mechanism mediated by thermal energy. The newfound prevalence of this structure occurring via nature in a biological system is grounds for mechanistic studies as well as phylogeny studies into the ancestry and branching of such a mechanism.

References

(1) Perez-Benito, J. F. Some Considerations on the Fundamentals of Chemical Kinetics: Steady State, Quasi-Equilibrium, and Transition State Theory. *J. Chem. Educ.* **2017**, *94* (9), 1238–1246. https://doi.org/10.1021/acs.jchemed.6b00957.

(2) Schowen, R. L. How an Enzyme Surmounts the Activation Energy Barrier. *Proc. Natl. Acad. Sci.* **2003**, *100* (21), 11931–11932. https://doi.org/10.1073/pnas.2235806100.

(3) Edwards, D. R.; Lohman, D. C.; Wolfenden, R. Catalytic Proficiency: The Extreme Case of S–O Cleaving Sulfatases. *J. Am. Chem. Soc.* **2012**, *134* (1), 525–531. https://doi.org/10.1021/ja208827q.

(4) Offenbacher, A. R.; Holman, T. R. Fatty Acid Allosteric Regulation of C-H Activation in Plant and Animal Lipoxygenases. *Molecules* **2020**, *25* (15), 3374. https://doi.org/10.3390/molecules25153374.

(5) Horitani, M.; Offenbacher, A. R.; Carr, C. A. M.; Yu, T.; Hoeke, V.; Cutsail, G. E.; Hammes-Schiffer, S.; Klinman, J. P.; Hoffman, B. M. ^{13} C ENDOR Spectroscopy of Lipoxygenase–Substrate Complexes Reveals the Structural Basis for C–H Activation by Tunneling. *J. Am. Chem. Soc.* **2017**, *139* (5), 1984–1997. https://doi.org/10.1021/jacs.6b11856.

(6) Meyer, M. P.; Tomchick, D. R.; Klinman, J. P. Enzyme Structure and Dynamics Affect Hydrogen Tunneling: The Impact of a Remote Side Chain (I553) in Soybean Lipoxygenase-1. *Proc. Natl. Acad. Sci.* **2008**, *105* (4), 1146–1151. https://doi.org/10.1073/pnas.0710643105.

(7) Knapp, M. J.; Rickert, K.; Klinman, J. P. Temperature-Dependent Isotope Effects in Soybean Lipoxygenase-1: Correlating Hydrogen Tunneling with Protein Dynamics. *J. Am. Chem. Soc.* **2002**, *124* (15), 3865–3874. https://doi.org/10.1021/ja012205t.

(8) Skrzypczak-Jankun, E.; Jankun, J.; Al-Senaidy, A. Human Lipoxygenase: Developments in Its Structure, Function, Relevance to Diseases and Challenges in Drug Development. *Curr. Med. Chem.* **2012**, *19* (30), 5122–5127. https://doi.org/10.2174/092986712803530520.

(9) Singh, P.; Arif, Y.; Miszczuk, E.; Bajguz, A.; Hayat, S. Specific Roles of Lipoxygenases in Development and Responses to Stress in Plants. *Plants* **2022**, *11* (7), 979. https://doi.org/10.3390/plants11070979.

(10) Offenbacher, A. R.; Iavarone, A. T.; Klinman, J. P. Hydrogen–Deuterium Exchange Reveals Long-Range Dynamical Allostery in Soybean Lipoxygenase. *J. Biol. Chem.* **2018**, *293* (4), 1138–1148. https://doi.org/10.1074/jbc.M117.817197.

(11) Newcomer, M. E.; Brash, A. R. The Structural Basis for Specificity in Lipoxygenase Catalysis: Specificity in Lipoxygenases. *Protein Sci.* **2015**, *24* (3), 298–309. https://doi.org/10.1002/pro.2626.

(12) Liu, S.; Han, B. Differential Expression Pattern of an Acidic 9/13-Lipoxygenase in Flower Opening and Senescence and in Leaf Response to Phloem Feeders in the Tea Plant. *BMC Plant Biol.* **2010**, *10* (1), 228. https://doi.org/10.1186/1471-2229-10-228.

(13) Zaragoza, J. P. T.; Offenbacher, A. R.; Hu, S.; Gee, C. L.; Firestein, Z. M.; Minnetian, N.; Deng, Z.; Fan, F.; Iavarone, A. T.; Klinman, J. P. Temporal and Spatial Resolution of Distal Protein Motions That Activate Hydrogen Tunneling in Soybean Lipoxygenase. *Proc. Natl. Acad. Sci.* **2023**, *120* (10), e2211630120. https://doi.org/10.1073/pnas.2211630120.

(14) Oliw, E. H. Iron and Manganese Lipoxygenases of Plant Pathogenic Fungi and Their Role in Biosynthesis of Jasmonates. *Arch. Biochem. Biophys.* **2022**, *722*, 109169. https://doi.org/10.1016/j.abb.2022.109169.

(15) Tzafriri, A. Michaelis–Menten Kinetics at High Enzyme Concentrations. *Bull. Math. Biol.* **2003**, *65* (6), 1111–1129. https://doi.org/10.1016/S0092-8240(03)00059-4.
(16) Lu, C.-Y.; Hsieh, K.-Y.; Liu, R. Future Challenges of Flash Memory Technologies. *Microelectron. Eng.* **2009**, *86* (3), 283–286. https://doi.org/10.1016/j.mee.2008.08.007.
(17) Burkard, G.; Gullans, M. J.; Mi, X.; Petta, J. R. Superconductor–Semiconductor Hybrid-Circuit Quantum Electrodynamics. *Nat. Rev. Phys.* **2020**, *2* (3), 129–140. https://doi.org/10.1038/s42254-019-0135-2.
(18) De Leon, N. P.; Itoh, K. M.; Kim, D.; Mehta, K. K.; Northup, T. E.; Paik, H.; Palmer, B. S.; Samarth, N.; Sangtawesin, S.; Steuerman, D. W. Materials Challenges and Opportunities for Quantum Computing Hardware. *Science* **2021**, *372* (6539), eabb2823. https://doi.org/10.1126/science.abb2823.
(19) Novoselov, K. S.; Jiang, Z.; Zhang, Y.; Morozov, S. V.; Stormer, H. L.; Zeitler, U.; Maan, J. C.; Boebinger, G. S.; Kim, P.; Geim, A. K. Room-Temperature Quantum Hall Effect in Graphene. *Science* **2007**, *315* (5817), 1379–1379. https://doi.org/10.1126/science.1137201.
(20) Anders, J.; Giovannetti, V. Thermodynamics of Discrete Quantum Processes. *New J. Phys.* **2013**, *15* (3), 033022. https://doi.org/10.1088/1367-2630/15/3/033022.
(21) Hughes, C.; Finke, D.; German, D.-A.; Merzbacher, C.; Vora, P. M.; Lewandowski, H. J. Assessing the Needs of the Quantum Industry. *IEEE Trans. Educ.* **2022**, *65* (4), 592–601. https://doi.org/10.1109/TE.2022.3153841.
(22) Aiello, C. D.; Awschalom, D. D.; Bernien, H.; Brower, T.; Brown, K. R.; Brun, T. A.; Caram, J. R.; Chitambar, E.; Di Felice, R.; Edmonds, K. M.; Fox, M. F. J.; Haas, S.; Holleitner, A. W.; Hudson, E. R.; Hunt, J. H.; Joynt, R.; Koziol, S.; Larsen, M.; Lewandowski, H. J.; McClure, D. T.; Palsberg, J.; Passante, G.; Pudenz, K. L.; Richardson, C. J. K.; Rosenberg, J. L.; Ross, R. S.; Saffman, M.; Singh, M.; Steuerman, D. W.; Stark, C.; Thijssen, J.; Vamivakas, A. N.; Whitfield, J. D.; Zwickl, B. M. Achieving a Quantum Smart Workforce. *Quantum Sci. Technol.* **2021**, *6* (3), 030501. https://doi.org/10.1088/2058-9565/abfa64.
(23) Ritz, T. Quantum Effects in Biology: Bird Navigation. *Procedia Chem.* **2011**, *3* (1), 262–275. https://doi.org/10.1016/j.proche.2011.08.034.
(24) Kim, Y.; Bertagna, F.; D'Souza, E. M.; Heyes, D. J.; Johannissen, L. O.; Nery, E. T.; Pantelias, A.; Sanchez-Pedreño Jimenez, A.; Slocombe, L.; Spencer, M. G.; Al-Khalili, J.; Engel, G. S.; Hay, S.; Hingley-Wilson, S. M.; Jeevaratnam, K.; Jones, A. R.; Kattnig, D. R.; Lewis, R.; Sacchi, M.; Scrutton, N. S.; Silva, S. R. P.; McFadden, J. Quantum Biology: An Update and Perspective. *Quantum Rep.* **2021**, *3* (1), 80–126. https://doi.org/10.3390/quantum3010006.
(25) Löwdin, P.-O. Proton Tunneling in DNA and Its Biological Implications. *Rev. Mod. Phys.* **1963**, *35* (3), 724–732. https://doi.org/10.1103/RevModPhys.35.724.
(26) Brookes, J. C. Quantum Effects in Biology: Golden Rule in Enzymes, Olfaction, Photosynthesis and Magnetodetection. *Proc. R. Soc. Math. Phys. Eng. Sci.* **2017**, *473* (2201), 20160822. https://doi.org/10.1098/rspa.2016.0822.
(27) Allen, W. E.; Hosbein, K. N.; Kennedy, A. M.; Whiting, B.; Walker, J. P. Design and Implementation of an Organic to Analytical CURE Sequence. *J. Chem. Educ.* **2021**, *98* (7), 2199–2208. https://doi.org/10.1021/acs.jchemed.1c00129.
(28) Corwin, L. A.; Graham, M. J.; Dolan, E. L. Modeling Course-Based Undergraduate Research Experiences: An Agenda for Future Research and Evaluation. *Cell Biol. Educ.* **2015**, *14* (1), es1–es1. https://doi.org/10.1187/cbe.14-10-0167.
(29) Goodwin, E. C.; Anokhin, V.; Gray, M. J.; Zajic, D. E.; Podrabsky, J. E.; Shortlidge, E. E. Is This Science? Students' Experiences of Failure Make a Research-Based Course Feel Authentic. *CBE—Life Sci. Educ.* **2021**, *20* (1), ar10. https://doi.org/10.1187/cbe.20-07-0149.

(30) Walker, J. P.; Allen, W. E.; Clevenger, L.; Hosbein, K. N.; Kennedy, A. M.; Vance-Chalcraft, H.; Whiting, B. Course-Based Undergraduate Research Experiences as a Community of Practice (CoP). *J. Chem. Educ.* **2023**, *100* (7), 2520–2528. https://doi.org/10.1021/acs.jchemed.2c00844.
(31) Satusky, M. J.; Wilkins, H.; Hutson, B.; Nasiri, M.; King, D. E.; Erie, D. A.; Freeman, T. C. CUREing Biochemistry Lab Monotony. *J. Chem. Educ.* **2022**, *99* (12), 3888–3898. https://doi.org/10.1021/acs.jchemed.2c00357.
(32) Wilczek, L. A.; Clarke, A. J.; Guerrero Martinez, M. del C.; Morin, J. B. Catalyzing the Development of Self-Efficacy and Science Identity: A Green Organic Chemistry CURE. *J. Chem. Educ.* **2022**, *99* (12), 3878–3887. https://doi.org/10.1021/acs.jchemed.2c00352.
(33) Heller, S. T.; Duncan, A. P.; Moy, C. L.; Kirk, S. R. The Value of Failure: A Student-Driven Course-Based Research Experience in an Undergraduate Organic Chemistry Lab Inspired by an Unexpected Result. *J. Chem. Educ.* **2020**, *97* (10), 3609–3616. https://doi.org/10.1021/acs.jchemed.0c00829.
(34) Hathaway, Russel S.; Nagda, Biren A.; Gregerman, Sandra R. The Relationship of Undergraduate Research Participation to Graduate and Professional Education Pursuit: An Empirical Study. *J. Coll. Stud. Dev.* **2002**, *43* (5), 1–18.
(35) Rodenbusch, S. E.; Hernandez, P. R.; Simmons, S. L.; Dolan, E. L. Early Engagement in Course-Based Research Increases Graduation Rates and Completion of Science, Engineering, and Mathematics Degrees. *CBE—Life Sci. Educ.* **2016**, *15* (2), ar20. https://doi.org/10.1187/cbe.16-03-0117.
(36) Szteinberg, G. A.; Weaver, G. C. Participants' Reflections Two and Three Years after an Introductory Chemistry Course-Embedded Research Experience. *Chem Educ Res Pr.* **2013**, *14* (1), 23–35. https://doi.org/10.1039/C2RP20115A.
(37) Blumling, D. E.; Hughey, C. A.; Boardman, B. M.; Judd, O. H.; Berndsen, C. E.; Boeckmann, D. M.; Paunovic, D. M.; Poe, T. M. Looking to Move Away from Expository General Chemistry Laboratories? We May Have a Cure for What "Ales" You. *J. Chem. Educ.* **2022**, *99* (12), 3858–3870. https://doi.org/10.1021/acs.jchemed.2c00363.
(38) Connor, M. C.; Pratt, J. M.; Raker, J. R. Goals for the Undergraduate Instructional Inorganic Chemistry Laboratory When Course-Based Undergraduate Research Experiences Are Implemented: A National Survey. *J. Chem. Educ.* **2022**, *99* (12), 4068–4078. https://doi.org/10.1021/acs.jchemed.2c00267.
(39) Strausser, S.; Bietsch, J.; Hodges, H.; McCoy, T.; Stewart, B.; Kintz, H.; Yeagley, A. An Organic Laboratory Experience: Synthesis and Antimicrobial Screening of Brominated Parabens. *J. Chem. Educ.* **2021**, *98* (11), 3524–3532. https://doi.org/10.1021/acs.jchemed.1c00355.
(40) Craig, P. A. A Survey on Faculty Perspectives on the Transition to a Biochemistry Course-Based Undergraduate Research Experience Laboratory: Transition to a CURE. *Biochem. Mol. Biol. Educ.* **2017**, *45* (5), 426–436. https://doi.org/10.1002/bmb.21060.
(41) Irby, S. M.; Pelaez, N. J.; Anderson, T. R. How to Identify the Research Abilities That Instructors Anticipate Students Will Develop in a Biochemistry Course-Based Undergraduate Research Experience (CURE). *CBE—Life Sci. Educ.* **2018**, *17* (2), es4. https://doi.org/10.1187/cbe.17-12-0250.
(42) Craig, P. A.; Anderson, T.; Bernstein, H. J.; Daubner, C.; Goodman, A.; Irby, S. M.; Koeppe, J.; Mills, J. L.; Pikaart, M.; Ringer McDonald, A.; others. Using Protein Function Prediction to Promote Hypothesis-Driven Thinking in Undergraduate Biochemistry Education. *Chemist* **2018**, *91* (1).
(43) Ritz, T.; Damjanović, A.; Schulten, K. The Quantum Physics of Photosynthesis. *ChemPhysChem* **2002**, *3* (3), 243. https://doi.org/10.1002/1439-7641(20020315)3:3<243::AID-CPHC243>3.0.CO;2-Y.
(44) Zaragoza, J. P. T.; Nguy, A.; Minnetian, N.; Deng, Z.; Iavarone, A. T.; Offenbacher, A. R.; Klinman, J. P. Detecting and Characterizing the Kinetic Activation of Thermal Networks in Proteins: Thermal Transfer from a Distal, Solvent-Exposed Loop to the Active Site in Soybean Lipoxygenase. *J. Phys. Chem. B* **2019**, *123* (41), 8662–8674. https://doi.org/10.1021/acs.jpcb.9b07228.

(45) *East Carolina University*. Carnegie Classification of Institutions of Higher Learning. https://carnegieclassifications.acenet.edu/institution/east-carolina-university/.
(46) Varadi, M.; Anyango, S.; Deshpande, M.; Nair, S.; Natassia, C.; Yordanova, G.; Yuan, D.; Stroe, O.; Wood, G.; Laydon, A.; Žídek, A.; Green, T.; Tunyasuvunakool, K.; Petersen, S.; Jumper, J.; Clancy, E.; Green, R.; Vora, A.; Lutfi, M.; Figurnov, M.; Cowie, A.; Hobbs, N.; Kohli, P.; Kleywegt, G.; Birney, E.; Hassabis, D.; Velankar, S. AlphaFold Protein Structure Database: Massively Expanding the Structural Coverage of Protein-Sequence Space with High-Accuracy Models. *Nucleic Acids Res.* **2022**, *50* (D1), D439–D444. https://doi.org/10.1093/nar/gkab1061.
(47) Mariani, V.; Biasini, M.; Barbato, A.; Schwede, T. lDDT: A Local Superposition-Free Score for Comparing Protein Structures and Models Using Distance Difference Tests. *Bioinformatics* **2013**, *29* (21), 2722–2728. https://doi.org/10.1093/bioinformatics/btt473.
(48) Knapp, M. J.; Klinman, J. P. Kinetic Studies of Oxygen Reactivity in Soybean Lipoxygenase-1. *Biochemistry* **2003**, *42* (39), 11466–11475. https://doi.org/10.1021/bi0300884.
(49) Klinman, J. P.; Offenbacher, A. R.; Hu, S. Origins of Enzyme Catalysis: Experimental Findings for C–H Activation, New Models, and Their Relevance to Prevailing Theoretical Constructs. *J. Am. Chem. Soc.* **2017**, *139* (51), 18409–18427. https://doi.org/10.1021/jacs.7b08418.